View metadata, citation and similar papers at core.ac.uk

brought to you by CORE

provided by Nottingham ePrints

The University of Nottingham

UNITED KINGDOM · CHINA · MALAYSIA

Gschwandtner, Martha and Piccinini, Anna Maria and Geriza, Tanja and Adage, Tiziana and Kungl, Andreas (2016) Interfering with the CCL2–glycosaminoglycan axis as a potential approach to modulate neuroinflammation. Neuroscience Letters, 626 . pp. 164-173. ISSN 1872-7972

Access from the University of Nottingham repository:
http://eprints.nottingham.ac.uk/46751/1/20160503_Gschwandtner_etal_revised02.pdf

Copyright and reuse:

The Nottingham ePrints service makes this work by researchers of the University of Nottingham available open access under the following conditions.

This article is made available under the University of Nottingham End User licence and may be reused according to the conditions of the licence. For more details see:
http://eprints.nottingham.ac.uk/end_user_agreement.pdf

A note on versions:

The version presented here may differ from the published version or from the version of record. If you wish to cite this item you are advised to consult the publisher's version. Please see the repository url above for details on accessing the published version and note that access may require a subscription.

For more information, please contact eprints@nottingham.ac.uk

Interfering with the CCL2 – glycosaminoglycan axis as a potential approach to modulate neuroinflammation

Martha Gschwandtner[a], Anna Maria Piccinini[b,1], Tanja Gerlza[b], Tiziana Adage[b], Andreas J. Kungl[a,b,*]

[a]Institute of Pharmaceutical Sciences, University of Graz, Schubertstraße 1/1, A- 8010 Graz, Austria

[b]ProtAffin Biotechnologie AG, A- 8020 Graz, Austria

[1]present address: School of Pharmacy, University of Nottingham, University Park, Nottingham, NG7 2RD, UK

*Address correspondence to this author at the Institute of Pharmaceutical Sciences, Department of Pharmaceutical Chemistry, University of Graz, Schubertstraße 1/1, 8010, Graz, Austria, Tel.: +43 316 380 5373, E-mail: andreas.kungl@uni-graz.at

Graphical Abstract

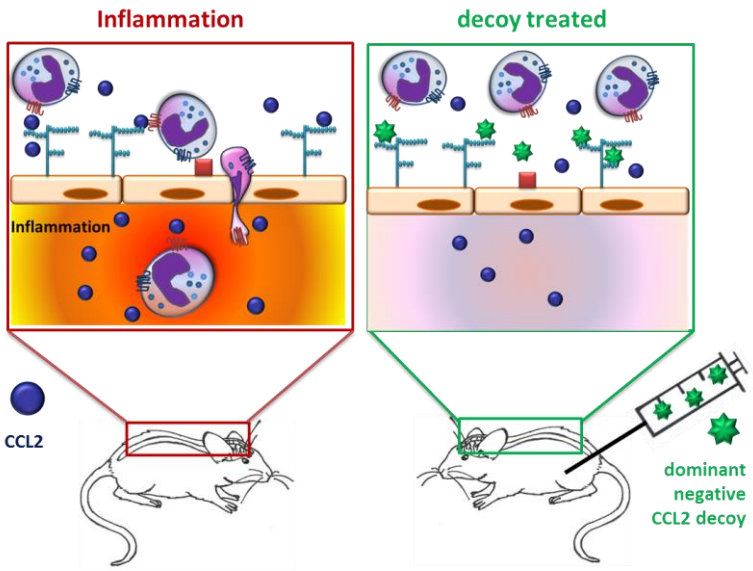

Abbreviations: MCP-1/CCL2, monocyte chemoattractant protein-1/; GPCR, G-protein coupled receptor; GAG, glycosaminoglycan, ECM, extracellular matrix; EAE, experimental autoimmune encephalomyelitis; MS, Multiple Sclerosis; CNS, central nervous system; MOG, myelin-oligodendrocyte-glycoprotein

Abstract

Multiple Sclerosis, a chronic inflammatory demyelinating disease of the central nervous system, ~~has been related with~~ involves increased expression of monocyte chemotactic protein 1 MCP1-/CCL2. For exerting its chemotactic effects, chemokine binding to glycosaminoglycans (GAGs) is required and therefore this interaction represents a potential target for therapeutic intervention. ~~Intending to engineer pro-inflammatory CCL2 towards an anti-inflammatory compound, we have designed a decoy variant, Met-CCL2 (Y13A S21K Q23R), embodying~~ We have designed an anti-inflammatory decoy variant, Met-CCL2 (Y13A S21K Q23R), embodying increased affinity for GAGs as well as knocked-out GPCR activation properties. This non-signalling dominant-negative mutant is shown here to be able to displace wild type CCL2 from GAGs by which it is supposed to interfere with the chemokine-related inflammatory response. *In vivo*, the anti-inflammatory properties were successfully demonstrated in a murine model of zymosan-induced peritonitis as well as in an experimental autoimmune encephalomyelitis, a model relevant for multiple sclerosis, where the compound lead to significantly reduced clinical scores due to reduction of cellular infiltrates and demyelination in spinal cord and cerebellum. These findings indicate a promising potential for future therapeutic development.

Keywords: CCL2 decoy, glycosaminoglycans, anti-inflammatory, Multiple Sclerosis, experimental autoimmune encephalomyelitis

1. Introduction

Chemokines are small secreted proteins that direct leukocyte trafficking from the lumen of blood vessels into the inflamed surrounding tissue [1]. Bound to glycosaminoglycans (GAGs, see below) on the endothelium, chemokines are retained at the site of action and are presented in their active conformation towards the attracted leukocytes [2]. Once activated *via* chemokine-specific GPCRs, the target blood cells migrate through the endothelial blood vessel cell layer to enter the site of tissue inflammation and to further induce and to boost the host immune response [3].

Monocyte chemoattractant protein-1 (MCP-1/CCL2) is a member of the chemokine-β family (CC chemokines), specifically activates monocytes and lymphocytes and is found in a variety of diseases that feature a monocyte-rich inflammatory component, such as atherosclerosis [4], rheumatoid arthritis [5] and congestive heart failure [6]. Most notably, there is also evidence that CCL2 plays a crucial role in the disease pathogenesis of Multiple Sclerosis (MS) [7, 8].

MS is an inflammatory disease of the central nervous system (CNS). It is caused by infiltrating leukocytes damaging myelin and axons, ultimately leading to extensive and chronic neurodegeneration [9, 10]. In this context, CCL2 is described to be responsible for CCR2-bearing leukocyte infiltration into the MS lesions of the CNS, but also for T-cell and monocyte migration within the CNS parenchyma. Moreover, CCL2 expression is altered depending on disease activity [11]. Particularly important is the reported observation that in active demyelinating as well as in chronic active MS lesions, reactive hypertrophic astrocytes are strongly immunoreactive for CCL2, suggesting a significant role for CCL2 in the recruitment and activation of myelin-degrading macrophages and thereby contributing to the evolution of MS [12]. Perivascular and parenchymal foamy macrophages do not express CCL2 protein and are likely to contribute to resolution of inflammation by inhibiting further lesion development and promoting lesion repair [13, 14]. On this line of evidence it has recently been reported that in a murine model of experimental autoimmune encephalomyelitis, mice with conditional astroglial ablation of CCL2 showed a reduced severity of pathology due to less spinal cord axonal loss [15]~~(Moreno et al. 2014)~~. Additionally, CCL2 significantly increases the permeability of the blood-brain barrier *in vivo* and thereby facilitates leukocyte migration during inflammation [16].

As mentioned above, chemokine activity *in vivo* was shown to be dependent on the interaction with glycosaminoglycans (GAGs) [2]. This means, that only the triple complex consisting of chemokine, chemokine-specific GPC receptor, and GAG co-receptor gives the fully functional entity for chemotaxis *in vivo*. These particular glycans are linear, negatively charged polysaccharides which consist of repeating disaccharide units of an amino sugar and a uronic acid [17]. Most of them are covalently attached to a core protein to form the so-

Commented [A1]: Reference inserted

Formatted: Font color: Red

Formatted: Font color: Red

called proteoglycans localized in the cell membrane or in the extracellular matrix [18]. The physiologically most relevant GAG types on cell surfaces and in the extracellular matrix are heparan sulfate and chondroitin sulfate which differ from one another in the disaccharide unit composition, the chain length and the degree of sulfation [19]. In fact, post-polymerization modifications, which include N-, 2-O, and 6-O sulfation as well as epimerization of GlcA into IdoA, provide high structural complexity within GAGs and allow the generation of particular oligosaccharide sequences that are supposed to be specific for their protein ligands, as it has been shown for antithrombin [20] and for basic fibroblast growth factor [21]. The sulfation patterns are cell type and tissue specific and are tightly regulated developmentally and pathophysiologically [22-24]. In the CNS GAGs/ proteoglycans can be found as ECM components and in the basement membrane [25, 26]. Although specificity/ selectivity in the chemokine/GAG interaction has not been fully elucidated so far, the great variety in GAG structures on the one side and the reported different affinities for GAGs displayed towards chemokines on the other side, suggest that chemokines interact with disease specific GAG structures *in vivo* [27, 28].

Applying a rational design approach based the CellJammer® Technology[29] human pro-inflammatory ~~CCL2 was turned into an anti-inflammatory chemokine decoy~~ CCL2 was altered to an anti-inflammatory chemokine decoy protein with increased glycan binding affinity, as previously reported by Piccinini et al. [30] and was shown to limit neointima formation and myocardial ischemia/ reperfusion injury in mice [31].

In this letter we describe the investigation of the anti-inflammatory activity of Met-CCL2 (Y13A S21K Q23R) in animals using the mechanistic inflammatory model of zymosan-induced peritonitis as well as a disease relevant model of Multiple Sclerosis, the experimental autoimmune encephalomyelitis (EAE).

Commented [A2]: New reference was inserted

Formatted: Font color: Red

2. Materials and Methods

2.1. Design, Expression and Purification

The CCL2 decoy Met-CCL2 (Y13A S21K Q23R) was designed on the basis of human mature CCL2 (1-76) (Swiss-Prot # P13500) by introducing 3 mutations in order to abolish receptor binding (Y13A) as well as to increase the affinity for its glycan ligand with additional positive amino acids (S21K Q23R) on both sides of the known GAG binding motif. Furthermore, Met-CCL2 constructs were generated in the background of a M64I mutation, which alters neither binding nor activity, however improves homogeneity of the mutants by eliminating the possibility of methionine sulfoxide species on position 64 [32]. The leading N-terminal Met residue is a result of the recombinant protein expression in *E. coli*. It was not cleaved off after expression since it did not compromise the heparan sulfate binding properties of the protein [30].

Met-CCL2 and Met-CCL2 (Y13A S21K Q23R) were expressed and purified as described previously [30]. During the purification process, good lab standard practices were applied to reduce endotoxin contents of protein samples by working with endotoxin-free plastic ware and by rinsing glass ware and chromatographic equipment with concentrated NaOH. The final bacterial endotoxin content of the chemokine mutant samples was determined by the limulus amebocyte lysate test (BioWhittaker, Cambrex). Typical values obtained were in the <0.18 EU/mL range.

2.2. ELISA-like Competition (ELICO)

2.5 µg GAG/ 250 nM biotinylated Met-CCL2 were diluted in PBS and coated onto Iduron (Manchester, UK) GAG-binding plates over night at RT. A washing step was performed to remove unbound biotinylated chemokine and GAG, followed by a 2 h incubation with different Met-CCL2 (Y13A S21K Q23R) concentrations diluted in PBS starting from 100 µM to 6 nM measuring each concentration in triplicates. To detect the remaining biotinylated Met-CCL2 we used an ELISA-like setup, therefore after another washing step we incubated the plates with high sensitivity Streptavidin HRP (Thermo Scientific, Waltham, MA, USA) diluted in 0.2 % dry milk that binds to the non-displaced biotinylated chemokine on the plate. After another hour incubation at RT and removal of unbound Streptavidin by a washing step, we analysed the plate by adding the substrate Tetramethylbenzidine (TMB), resulting in a blue colour change. After stopping the reaction with sulphuric acid the absorbance at 450 nm was read in a Beckman Coulter DTX 800 Multimode Detector (Beckman Coulter, Austria). The reference (OD620) values were subtracted from the sample values (OD450) and the Mean and Standard Deviation was calculated. Data analysis was performed using specialized statistical software Origin® (GE Healthcare, Chalfont St Giles, UK).

2.3. Animal experiments

Animal care and handling procedures were performed in accordance with the European guidelines and all the experiments received prior approval from the local ethics committees.

2.3.1. *Met-CCL2 (Y13A S21K Q23R) Pharmacokinetics*

Male C57BL/6 mice (SIPPR-BK Laboratory, Shanghai) were group housed under a 12:00 h light /dark cycle, provided with food and water ad libitum and allowed to acclimatize for at least 1 week before the experiment. Animals were treated with Met-CCL2 (Y13A S21K Q23R) at a dose of 40 µg/kg intravenously (i.v.) or at 40 µg/kg and 400µg/kg intrapritoneally (i.p.). At prefixed times post administration approximately 200 µL blood was collected via retro-orbital from deeply isoflurane anesthetized mice (n= 3/time/dose) and transferred to a centrifuge tube and kept on wet ice for 30 min. Serum was separated by centrifugation at

5,000 rpm for 15 minutes at 4ºC. The resulting serum was stored at -80ºC until subjected to ELISA for quantification. The ELISA (h-MCP-1, Anogen Cat. No.:EL0009) was validated for cross reactivity with Met-CCL2 (Y13A S21K Q23R) and performed according to the manufacturer's instructions. The lower limit of detection was 50 pg/ml.

2.3.2. Zymosan-Induced Peritonitis

Male C57BL/6 mice (Charles River, UK) were group housed under a 12:00 h light /dark cycle, provided with food and water *ad libitum* and allowed to acclimatize for at least 1 week before the experiment. On the experiment day, all the animals were injected with 0.2 mg of zymosan (Sigma-Aldrich) intraperitoneally (time 0) to induce peritonitis. Pharmacological treatments with vehicle (sterile PBS i.v. n=8), with dexamethasone (1 mg/kg s.c. n=8)or with Met-CCL2 (Y13A S21K Q23R) (40 µg/kg i.v. +n = 8) were performed 1h and 6 hours post zymosan injection. Sham animals (intraperitoneal treatment with saline n = 3) were used as controls. 24 hours post zymosan intraperitoneal administration, the peritoneal cavities were washed with 3 mL of PBS containing 3 mM EDTA and the number of total leukocytes was determined by staining with Turk's solution (0.01% crystal violet in 3% acetic acid) and counting using a Neubauer hemocytometer and a light microscope. Appropriate aliquots were then stained using specific antibodies (FITC GR-1 (Ly6G and Ly6C), clone RB6-8C5; APC F4/80; eBioscience) and flow cytometric analysis was performed using a FACScan analyzer (Becton Dickinson). Cells were initially characterized using the forward and side scatter characteristics, to distinguish between the three distinct cell populations (lymphocytes, monocytes / macrophages and granulocytes). Further gating was performed using cells collected in sham and zymosan + vehicle. Cells positive for Gr1 and negative for F4/80 determined the granulocyte population. Cells positive for F4/80 and negative for Gr1 determined the macrophage population. Cells positive for both antigens indicated the inflammatory monocyte population. Determination of positive and negative populations was performed based on the control staining with an irrelevant IgG isotype labeled with FITC or APC (both from eBioscience). Once determined, gating quadrants were rigorously maintained for the analyses of the cells all the groups. The experiment was repeated twice, and data from one experiment are presented.

2.3.3. MOG-Induced Experimental Autoimmune Encephalomyelitis (EAE)

Ten-week old, female C57BL/6 mice (Charles River, NL,) were group housed under a 12:00 h light /dark cycle, provided with food and water *ad libitum* and allowed to acclimatize for at least 2 weeks before the experiment. During the experiment additional mixture of powder food and water was given into the animal's cage. On day 0 and day 7 the mice were immunized with 200 µg MOG(35-55) (Isogen life science) in an emulsion of PBS and

complete Freund's adjuvant supplemented with *M. tuberculosis* H37RA (both Difco Laboratories) administered subcutaneously in both flanks. On day 0 and on day 2 the mice additionally received i.v. 300 ng Pertussis toxin (Calbiochem). Pharmacological interventions were administered from day from day 7 post immunization (n = 10/group) when no clinical signs of the pathology are present, but an increase in circulating chemokines (including murine CCL2, also known as JE) is already reported, and was continued once daily for 21 days (day 28 post immunization) The mice were treated with vehicle i.p., dexamethasone 1 mg/kg i.p., and 40, 200 and 400 µg/kg Met-CCL2 (Y13A S21K Q23R) i.p. During the experiment mice were monitored daily and body weight was recorded. EAE score was assessed daily using the following scoring system: 0 = no disease, 0.5 = tail paresis or partial paralysis, 1 = complete tail paralysis, 2 = paraparesis: limb weakness and tail paralysis, 2.5 = partial limb paralysis, 3 = complete hind- or front limb paralysis, 3.5 = paraplegia, 4 = quadriplegia, moribund, 5 = death due to EAE.These data were used also to determine the day of onset, defined as the first of three consecutive days on which a cumulative clinical score of at least three was reached, the maximum clinical score and the cumulative clinical score. On day 28 mice were euthanized and the central nervous system collected, fixed and stored in formaldehyde. Spinal cord and cerebellum of each mouse in the vehicle, dexamethasone and Met-CCL2 (Y13A S21K Q23R) 40 µg/kg groups were embedded in paraffin. Sections (5µm, separated by 50µm) were generated and stained using Hematoxylin/Eosin and scored for cellular infiltrates or stained using Kluver-Barrera and assessed for demyelinization. In both cases a minimum of three slides/animals/tissue were quantified using a qualitative scale of 0 to 4.

2.4. Statistical analysis

All data are reported as means ± standard errors of the means (SEM). Pharmacokinetic profiles of Met-CCL2 (Y13A S21K Q23R) were evaluated with WinNonLin using non-compartment model. For the zymosan-induced peritonitis, statistical analysis was performed using ANOVA followed by Dunnett's multiple comparison using GraphPad Prism software. The EAE data were analyzed using the Kruskal-Wallis test followed by the Mann-Whitney U-test. The significance of differences between the treatment groups in the time-dependent outcome parameters (daily clinical score and body weight) were tested using repeated-measures ANOVA, followed by LSD post hoc. Analysis was performed using SPSS17 for Windows. In both cases, the significance level was set at $p<0.05$. Significance is reported as follows: * $p<0.05$; ** $p<0.01$; *** $p<0.01$.

3. **Results**

3.1. ELISA-Like Competition Assay

Since our mutant proteins were designed in a way to displace the corresponding wild type chemokine from its GAG co-receptor, we have developed a novel competition assay which gives IC_{50} values derived from displacement curves rather than K_d values obtained from bi-molecular binding isotherms [33]. In our assay we have tried to mimic the glycocalyx of cell surfaces by coating heparan sulfate onto specially prepared microtiter plates. We then added biotinylated Met-CCL2 which was, after washing, displaced either by unmodified Met-CCL2 or by Met-CCL2 (Y13A S21K Q23R) in a concentration-dependent manner (Figure 1). The IC_{50} values derived from these experiments clearly show that the mutant chemokine is a much better competitor for bound Met-CCL2 (giving an IC_{50} value of 740 nM) than unmodified Met-CCL2 (IC_{50} = 3092 nM).

Commented [A3]: New reference inserted (instead of 28)

Formatted: Font color: Red

3.2. Met-CCL2 (Y13A S21K Q23R) Pharmacokinetics

Pharmacokinetic profiles of Met-CCL2 (Y13A S21K Q23R) after i.v. and i.p. administration are shown in Figure 2. After i.v. administration the protein was eliminated, as expected, relatively fast, with a serum half-life ($t_{1/2}$) of 1.08 h, and an area under the curve ($AUC_{0\text{-last}}$) of 22.3 h*ng/mL. After i.p. administration at 40µg/kg the protein was absorbed with a time of maximal concentration (T_{max}) of 15 min, the maximal serum concentration (C_{max}) of 0.69 ng/ml and the $AUC_{0\text{-last}}$ of 4.86 h*ng/mL, the $t_{1/2}$ was of 1.75 h. After i.p. administration at 400µg/kg the protein was absorbed with T_{max} of 1 h at a C_{max} of 19.9 ng/ml and the $AUC_{0\text{-last}}$ of 473 h*ng/mL, the $t_{1/2}$ was of 4.13 h,. No levels were detectable in the 24 h samples of mice treated i.v. or i.p. at the dose of 40µg/kg.

3.3. Zymosan-Induced Peritonitis

In this study Met-CCL2 (Y13A S21K Q23R) at a concentration of 40 µg/kg i.v. was directly compared to the immunosuppressant dexamethasone at a dose of 1 mg/kg s.c. While the latter reduced the total cell infiltrate (data not shown), Met-CCL2 (Y13A S21K Q23R) effects were specifically observed on a particular subset of monocytes expressing F4/80 as well as Gr1 (Ly6C and Ly6G) marker, and considered to be a pro-inflammatory subset of monocytes (Figure 3A R5 and 3C) , while not affecting the number of residential macrophages ($F4/80^{high}/Gr1^{-ve}$, Figure 3A R3-4 and 3B), that are thought to contribute to the pathology resolution [34].

3.4. MOG-Induced Experimental Autoimmune Encephalomyelitis (EAE)

Immunization with the MOG(35-55) protein successfully induced EAE in vehicle treated animals, with an incidence of 100%. In our study, administration of 40, 200 and 400 µg/kg of Met-CCL2 (Y13A S21K Q23R) i.p. from day 7 post immunization onwards significantly delayed the day of onset of the disease independently of the dose (Figure 4B) and resulted

in an overall better clinical score (Figure 4A), a reduced maximal disease severity (Figure 3b), and a cumulative clinical score (Figure 4C). Additionally, Met-CCL2 (Y13A S21K Q23R) promoted preservation of body weight (Figure 5A) and increased survival (Figure 5B). In EAE animals, where progressive paralysis reduces animal motility and impacts the ability of the animals to feed, even if food if provided into the cage, a diminished loss of body weight is considered to reflect an index of animal general well-being.

Histological analysis showed that compared to the vehicle-treated control group Met-CCL2 (Y13A S21K Q23R) and dexamethasone significantly reduced the influx of inflammatory cells to the cerebellum and the spinal cord, (cerebellum: vehicle 1.55 ± 0.3, Met-CCL2 (Y13A S21K Q23R) 0.35 ± 0.1***, dexamethasone 0.1 ± 0.2***; spinal cord: vehicle 1.81 ± 0.4, Met-CCL2 (Y13A S21K Q23R) 0.33 ± 0.1***, dexamethasone0.37+0.17*** see Figure 6 A-H) as well as demyelination (cerebellum: vehicle 1.33 ± 0.4, Met-CCL2 (Y13A S21K Q23R) 0.44 ± 0.2, dexamethasone 0.08 ± 0.03; spinal cord: vehicle 3.3 ± 0.3, Met-CCL2 (Y13A S21K Q23R) 0.63 ± 0.2, dexamethasone 0.63 ± 0.3 see Figure 7 A-H).

4. Discussion

Met-CCL2 (Y13A S21K Q23R) shows higher GAG binding affinity compared to Met-CCL2 but shows impaired CCR2 receptor activation [30]. Here we show that, in addition, the mutant is able to displace the wild type chemokine efficiently from HS chains (see Figure 1). Since it is proposed that CCL2 *in vivo* is mainly displayed to approaching monocytes/macrophages in a GAG-bound form, the competitive potency (expressed in the IC_{50} value) of a CCL2 mutant is much more relevant parameter than the direct binding of chemokine to its GAG ligand. This relates directly to the proposed mode of action of the CCL2 mutant, namely that it acts like a protein-based GAG antagonist.

The proposed anti-inflammatory effect of the mutant was subsequently tested *in vivo* in a mechanistic model of zymosan- induced peritonitis [35] to allow initial assessment of the dose *in vivo* and anti-inflammatory/anti-migratory properties, and only then in an animal model of multiple sclerosis, EAE. ~~the experimental autoimmune encephalomyelitis (EAE).~~

In the zymosan- induced peritonitis model we could show that we are able to retain selectivity for the specific cell populations *in vivo*, thereby selectively inhibiting the recruitment of Gr1 and F4/80 double positive cells, considered to be newly recruited inflammatory monocytes, while not affecting macrophages~~the macrophage number~~. Moreover, this finding implies that the mutant has found its appropriate endothelial GAG target and gained the energetically preferred active form.

MOG-induced EAE in mice is recognized to be a good experimental model of human MS pathogenesis [7, 36, 37], and in the present study MOG(35-55) successfully induced EAE in all vehicle treated animals. The severity of the pathology caused death in some animals. By

administering the decoy molecule the disease onset could be delayed significantly. Furthermore, the maximal clinical score was significantly decreased showing differences in the maximal disease severity that are particularly relevant in terms of quality of life when translated to the human situation. The efficacy of the decoy molecule observed at clinical score level correlated, as expected, with changes at histological level in which~~where~~ vehicle-treated animals showed massive infiltration of inflammatory cells in the spinal cord and in the perivascular region of the cerebellum, whereas almost no inflammatory cell infiltrates were present in decoy treated animals. Moreover, the myelin exhibited normal features in decoy treated animals in contrast to pronounced demyelination in the spinal cord of vehicle-treated animals.

The observed effect could not be due to inhibition of bone marrow cell mobilization, as has been reported for inhibitors of the GPC receptor CCR2 [38, 39], since we have already shown that Met-CCL2 (Y13A S12K Q23R) does not bind or activate, CCR2 [30]. Surprisingly, Met-CCL2 (Y13A S12K Q23R) activity on the different parameters measured was not dose-dependent, with the lowest dose administered being the most effective. This is not due to a non-linear exposure, since the PK profile for the protein seems to be linear in this range (at least in term of AUC). The binding affinities of chemokines to GAGs are known to not be dose dependent~~be not dose dependent~~ [40] with loss of affinity at too high concentrations, therefore, even if it seems unlikely from the plasma concentration measured during the PK assessment, we cannot exclude that at the two higher doses the binding equilibrium at the GAG target was moving toward dissociation. Alternatively, it is possible that the apparent differences observed between doses are due to the limited number of animals used in the experiment, ~~where~~ in which even the survival of one more animal in a treatment group may affect the overall clinical score profile, suggesting that plateau activity is already achieved at a dose of 40µg/kg. This aspect should be further analyzed using a broader range of doses and in a time-course experiment, with direct assessment of cell type infiltrates in the CNS of the animals by either immunohistochemistry, or FACs analysis.

However, the clinical development of a protein requesting daily administration is not foreseeable (and already difficult to assess preclinically, since twice a day chronic treatment is not feasible in mice), and strategies to extend its exposure, such as by conjugation with carrier proteins (e.g. human serum albumin) are currently under evaluation [41] and will be further tested in MS animal models.

What we can state from the current data is that the dose of 40 µg/kg Met-CCL2 (Y13A S12K Q23R) was, in both the experimental peritonitis and in the EAE model, at least as effective as dexamethasone in reducing inflammation and consequent demyelination. It has to be

considered that dexamethasone was administered in this study at a dose highly effective in mice, but toxic if translated to a human dose.

In conclusion, we have confirmed that the engineered increased GAG binding affinity of Met-CCL2 (Y13A S21K Q23R), which was measured *in vitro*, can be translated into anti-inflammatory activities *in vivo*. Our approach of targeting glycans for interfering with CCL2 signalling in CNS inflammation is completely unique, and opens a possible new avenue for therapeutic intervention that may be applicable to MS treatment.

Acknowledgments

We would like to thank M. Perretti, T. Montero-Melendez and V. Brancaleone from William Harvey Research Institute (London UK), and F. Tielen from TNO (Leiden, The Netherlands). M. Gschwandtner is recipient of a DOC Fellowship of the Austrian Academy of Sciences at the Institute of Pharmaceutical Sciences, University of Graz.

References

[1] M. Baggiolini, Chemokines and leukocyte traffic, Nature, 392 (1998) 565-568.
[2] A.E.I. Proudfoot, T.M. Handel, Z. Johnson, E.K. Lau, P. LiWang, I. Clark-Lewis, F. Borlat, T.N.C. Wells, M.H. Kosco-Vilbois, Glycosaminoglycan binding and oligomerization are essential for the in vivo activity of certain chemokines, Proc. Natl. Acad. Sci. U. S. A., 100 (2003) 1885-1890.
[3] C.R. Parish, Heparan sulfate and inflammation, Nat. Immunol., 6 (2005) 861-862.
[4] J.R. Harrington, The Role of MCP-1 in Atherosclerosis, Stem Cells, 18 (2000) 65-66.
[5] M. Harigai, M. Hara, T. Yoshimura, E.J. Leonard, K. Inoue, S. Kashiwazaki, Monocyte chemoattractant protein-1 (MCP-1) in inflammatory joint diseases and its involvement in the cytokine network of rheumatoid synovium, Clin. Immunol. Immunopathol., 69 (1993) 83-91.
[6] P. Aukrust, T. Ueland, F. Müller, A.K. Andreassen, I. Nordøy, H. Aas, J. Kjekshus, S. Simonsen, S.S. Frøland, L. Gullestad, Elevated circulating levels of CC chemokines in patients with congestive heart failure, Circulation, 97 (1998) 1136-1143.
[7] L. Izikson, R.S. Klein, I.F. Charo, H.L. Weiner, A.D. Luster, Resistance to experimental autoimmune encephalomyelitis in mice lacking the CC chemokine receptor (CCR2), The Journal of experimental medicine, 192 (2000) 1075-1080.
[8] D.J. Mahad, R.M. Ransohoff, The role of MCP-1 (CCL2) and CCR2 in multiple sclerosis and experimental autoimmune encephalomyelitis (EAE), Semin. Immunol., Elsevier, 2003, pp. 23-32.
[9] A. Compston, A. Coles, Multiple sclerosis, Lancet, 372 (2008) 1502-1517.
[10] C.M. Poser, V.V. Brinar, Diagnostic criteria for multiple sclerosis, Clin. Neurol. Neurosurg., 103 (2001) 1-11.
[11] D. Mahad, S. Howell, M. Woodroofe, Expression of chemokines in the CSF and correlation with clinical disease activity in patients with multiple sclerosis, J. Neurol. Neurosurg. Psychiatry, 72 (2002) 498-502.
[12] R.-N.E. Dogan, A. Elhofy, W.J. Karpus, Production of CCL2 by central nervous system cells regulates development of murine experimental autoimmune encephalomyelitis through the recruitment of TNF-and iNOS-expressing macrophages and myeloid dendritic cells, The Journal of Immunology, 180 (2008) 7376-7384.

[13] P. Van Der Voorn, J. Tekstra, R.H. Beelen, C.P. Tensen, P. Van Der Valk, C.J. De Groot, Expression of MCP-1 by reactive astrocytes in demyelinating multiple sclerosis lesions, The American journal of pathology, 154 (1999) 45-51.
[14] C. McManus, J.W. Berman, F.M. Brett, H. Staunton, M. Farrell, C.F. Brosnan, MCP-1, MCP-2 and MCP-3 expression in multiple sclerosis lesions: an immunohistochemical and in situ hybridization study, J. Neuroimmunol., 86 (1998) 20-29.
[15] M. Moreno, P. Bannerman, J. Ma, F. Guo, L. Miers, A.M. Soulika, D. Pleasure, Conditional ablation of astroglial CCL2 suppresses CNS accumulation of M1 macrophages and preserves axons in mice with MOG peptide EAE, J. Neurosci., 34 (2014) 8175-8185.
[16] S.M. Stamatovic, P. Shakui, R.F. Keep, B.B. Moore, S.L. Kunkel, N. Van Rooijen, A.V. Andjelkovic, Monocyte chemoattractant protein-1 regulation of blood–brain barrier permeability, J. Cereb. Blood Flow Metab., 25 (2005) 593-606.
[17] J.D. Esko, U. Lindahl, Molecular diversity of heparan sulfate, J. Clin. Invest., 108 (2001) 169.
[18] J.R. Bishop, M. Schuksz, J.D. Esko, Heparan sulphate proteoglycans fine-tune mammalian physiology, Nature, 446 (2007) 1030-1037.
[19] K.K. Esko JD, Lindahl U, Proteoglycans and Sulfated Glycosaminoglycans., Essentials of Glycobiology, Cold Spring Harbor Laboratory Press2009.
[20] L. Jin, J.P. Abrahams, R. Skinner, M. Petitou, R.N. Pike, R.W. Carrell, The anticoagulant activation of antithrombin by heparin, Proceedings of the National Academy of Sciences, 94 (1997) 14683-14688.
[21] J.E. Turnbull, D. Fernig, Y. Ke, M.C. Wilkinson, J.T. Gallagher, Identification of the basic fibroblast growth factor binding sequence in fibroblast heparan sulfate, J. Biol. Chem., 267 (1992) 10337-10341.
[22] E. Feyzi, T. Saldeen, E. Larsson, U. Lindahl, M. Salmivirta, Age-dependent modulation of heparan sulfate structure and function, J. Biol. Chem., 273 (1998) 13395-13398.
[23] N.M. Carter, S. Ali, J.A. Kirby, Endothelial inflammation: the role of differential expression of N-deacetylase/N-sulphotransferase enzymes in alteration of the immunological properties of heparan sulphate, J. Cell Sci., 116 (2003) 3591-3600.
[24] R. Sasisekharan, Z. Shriver, G. Venkataraman, U. Narayanasami, Roles of heparan-sulphate glycosaminoglycans in cancer, Nature Reviews Cancer, 2 (2002) 521-528.
[25] E. Ruoslahti, Brain extracellular matrix, Glycobiology, 6 (1996) 489-492.
[26] J. Van Horssen, C.D. Dijkstra, H.E. De Vries, The extracellular matrix in multiple sclerosis pathology, J. Neurochem., 103 (2007) 1293-1301.
[27] G.S. Kuschert, F. Coulin, C.A. Power, A.E. Proudfoot, R.E. Hubbard, A.J. Hoogewerf, T.N. Wells, Glycosaminoglycans interact selectively with chemokines and modulate receptor binding and cellular responses, Biochemistry, 38 (1999) 12959-12968.
[28] J.D. Esko, S.B. Selleck, Order out of chaos: assembly of ligand binding sites in heparan sulfate, Annu. Rev. Biochem., 71 (2002) 435-471.
[29] T. Adage, A.-M. Piccinini, A. Falsone, M. Trinker, J. Robinson, B. Gesslbauer, A.J. Kungl, Structure-based design of decoy chemokines as a way to explore the pharmacological potential of glycosaminoglycans, Br. J. Pharmacol., 167 (2012) 1195-1205.
[30] A.M. Piccinini, K. Knebl, A. Rek, G. Wildner, M. Diedrichs-Möhring, A.J. Kungl, Rationally evolving MCP-1/CCL2 into a decoy protein with potent anti-inflammatory activity in vivo, J. Biol. Chem., 285 (2010) 8782-8792.
[31] E.A. Liehn, A.-M. Piccinini, R.R. Koenen, O. Soehnlein, T. Adage, R. Fatu, A. Curaj, A. Popescu, A. Zernecke, A.J. Kungl, A new monocyte chemotactic protein-1/chemokine CC motif ligand-2 competitor limiting neointima formation and myocardial ischemia/reperfusion injury in mice, J. Am. Coll. Cardiol., 56 (2010) 1847-1857.
[32] C.D. Paavola, S. Hemmerich, D. Grunberger, I. Polsky, A. Bloom, R. Freedman, M. Mulkins, S. Bhakta, D. McCarley, L. Wiesent, B. Wong, K. Jarnagin, T.M. Handel,

Monomeric monocyte chemoattractant protein-1 (MCP-1) binds and activates the MCP-1 receptor CCR2B, J. Biol. Chem., 273 (1998) 33157-33165.
[33] T. Gerlza, B. Hecher, D. Jeremic, T. Fuchs, M. Gschwandtner, A. Falsone, B. Gesslbauer, A.J. Kungl, A combinatorial approach to biophysically characterise chemokine-glycan binding affinities for drug development, Molecules, 19 (2014) 10618-10634.
[34] M.N. Ajuebor, A.M. Das, L. Virág, R.J. Flower, C. Szabó, M. Perretti, Role of resident peritoneal macrophages and mast cells in chemokine production and neutrophil migration in acute inflammation: evidence for an inhibitory loop involving endogenous IL-10, J. Immunol., 162 (1999) 1685-1691.
[35] J.L. Cash, G.E. White, D.R. Greaves, Zymosan-induced peritonitis as a simple experimental system for the study of inflammation, Methods Enzymol., 461 (2009) 379-396.
[36] M.K. Racke, Experimental autoimmune encephalomyelitis (EAE), Curr. Protoc. Neurosci., (2001) 9.7. 1-9.7. 11.
[37] K.J. Kennedy, R.M. Strieter, S.L. Kunkel, N.W. Lukacs, W.J. Karpus, Acute and relapsing experimental autoimmune encephalomyelitis are regulated by differential expression of the CC chemokines macrophage inflammatory protein-1α and monocyte chemotactic protein-1, J. Neuroimmunol., 92 (1998) 98-108.
[38] H. Jung, D.S. Mithal, J.E. Park, R.J. Miller, Localized CCR2 Activation in the Bone Marrow Niche Mobilizes Monocytes by Desensitizing CXCR4, PLoS One, 10 (2015) e0128387.
[39] Y. Wang, L. Cui, W. Gonsiorek, S.-H. Min, G. Anilkumar, S. Rosenblum, J. Kozlowski, D. Lundell, J.S. Fine, E.P. Grant, CCR2 and CXCR4 regulate peripheral blood monocyte pharmacodynamics and link to efficacy in experimental autoimmune encephalomyelitis, J Inflamm (Lond), 6 (2009) 32.
[40] B. Goger, Y. Halden, A. Rek, R. Mösl, D. Pye, J. Gallagher, A.J. Kungl, Different affinities of glycosaminoglycan oligosaccharides for monomeric and dimeric interleukin-8: a model for chemokine regulation at inflammatory sites, Biochemistry, 41 (2002) 1640-1646.
[41] T. Gerlza, S. Winkler, A. Atlic, C. Zankl, V. Konya, N. Kitic, E. Strutzmann, K. Knebl, T. Adage, A. Heinemann, R. Weis, A.J. Kungl, Designing a mutant CCL2-HSA chimera with high glycosaminoglycan-binding affinity and selectivity, Protein Eng. Des. Sel., 28 (2015) 231-240.

Figure Captions

Figure 1: ELICO displacement assay of Met-CCL2 (Y13A S21K Q23R) (black) in comparison to Met-CCL2 (grey) competing with biotinylated Met-CCL2 for binding to heparan sulfate. The normalized absorption values (mean+/-SD) at 450 nm (TMB) were plotted against the concentration of the proteins. IC_{50} values were determined by competition analysis of the displacement curves.

Figure 2: Pharmacokinetic profiles of Met-CCL2 (Y13A S21K Q23R) administered at the dose of 40µg/kg i.v. or 40 and 40µg/kg i.p. in male C57BL/6 mice. Serum levels were evaluated using a commercial h-MCP-1 ELISA validated to recognize our protein.

Figure 3: Zymosan-induced peritonitis in C57BL/6 male mice caused a strong infiltration of cells, which were characterized by FACS using the forward and side scatter characteristics. Further gating criteria were set using cells collected in sham (panel A left) and zymosan + vehicle (panel A right). FL-1 channel on x axis (Gr-1), FL4 on y axis (F4/80). $Gr1^{high}/F4/80^{-ve}$: granulocyte population (R2); $F4/80^{high}/Gr1^{-ve}$: macrophage (R3+R4); Cells positive for both antigens indicated the inflammatory monocyte population (R5). $Gr1^{high}/F4/80^{+ve}$ inflammatory monocytes. Based on this gating, dexamethasone showed activity on all cell types (B,C), while Met-CCL2 (Y13A S21K Q23R) showed specific activity on the inflammatory monocytes (C). Anova followed by ANOVA followed by Dunnett's multiple comparison. ** $p<0.01$; ***$p<0.001$.

Figure 4: MOG(35-55) EAE was induced in C57BL/6 female mice (n=10/group). Main parameters for disease severity are reported as follows, **A**: daily clinical score; data were analysed using repeated-measures ANOVA ($p<0.001$), followed by LSD: dexamethasone $p<0.001$, Met-CCL2 (Y13A S21K Q23R) 40µg/kg $p<0.001$, 200µg/kg and 400µg/kg$p<0.05$ vs vehicle treatment; **B**: day of disease onset; **C**: maximal clinical score, and **D**: cumulative clinical score. Kruskal-Wallis followed by Mann-Whitney U-test. *$p<0.05$; **$p<0.01$; ***$p<0.001$ vs Vehicle.

Figure 5: MOG(35-55) EAE was induced in C57BL/6 female mice. **A:** daily body weight data were analysed using repeated-measures ANOVA ($p<0.001$), followed by LSD: Met-CCL2 (Y13A S21K Q23R) 40µg/kg $p<0.001$. **B**: survival curves show up to a 30% mortality in the vehicle group, that was reduced by Met-CCL2 (Y13A S21K Q23R) treatment, with no dead animals in the 40µg/kg group.

Figure 6: Histological analysis of the MOG(35-55)-induced EAE C57BL/6 female mice euthanized at day 28 post immunization. Spinal cord and cerebellum of each mouse in the vehicle, dexamethasone and Met-CCL2 (Y13A S21K Q23R) 40 µg/kg groups were embedded in paraffin. Sections (5µm, separated by 50µm) were generated and stained using Hematoxylin/Eosin and scored for cellular infiltrates. Representative images at two different magnifications. : **A** vehicle cerebellum 4 x; **B** vehicle cerebellum 20 x; **C** vehicle spinal cord 4x; **D** vehicle spinal cord 20x; **E** Met-CCL2 (Y13A S21K Q23R) 40µg/kg cerebellum 4x; **F** Met-CCL2 (Y13A S21K Q23R) 40µg/kg cerebellum 20x; **G** Met-CCL2 (Y13A S21K Q23R) 40µg/kg spinal cord 4x; **H** Met-CCL2 (Y13A S21K Q23R) 40µg/kg spinal cord 4x. Animals in the dexamethasone groups presented similar features as animals in the Met-CCL2 (Y13A S21K Q23R) 40µg/kg group.

Figure 7: Histological analysis of the MOG(35-55)-induced EAE C57BL/6 female mice euthanized at day 28 post immunization. Spinal cord and cerebellum of each mouse in the vehicle, dexamethasone and Met-CCL2 (Y13A S21K Q23R) 40 µg/kg groups were embedded in paraffin. Sections (5µm, separated by 50µm) were generated and stained using Kluver-Barrera and assessed for demyelinization. Representative images at two different magnifications. : **A** vehicle cerebellum 4 x; **B** vehicle cerebellum 20 x; **C** vehicle spinal cord 4x; **D** vehicle spinal cord 20x; **E** Met-CCL2 (Y13A S21K Q23R) 40µg/kg cerebellum 4x; **F** Met-CCL2 (Y13A S21K Q23R) 40µg/kg cerebellum 20x; **G** Met-CCL2 (Y13A S21K Q23R) 40µg/kg spinal cord 4x; **H** Met-CCL2 (Y13A S21K Q23R) 40µg/kg spinal cord 4x. Animals in the dexamethasone groups presented similar features as animals in the Met-CCL2 (Y13A S21K Q23R) 40µg/kg group.

Figure 1

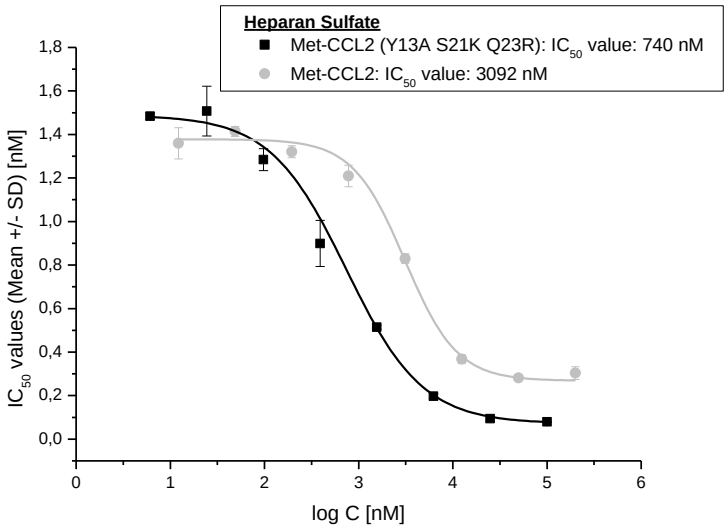

Figure 2

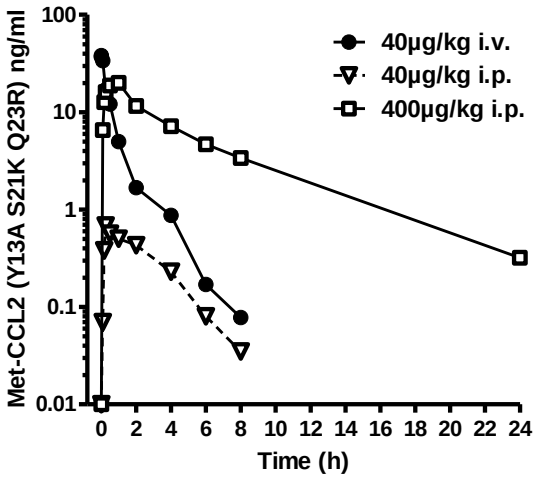

Figure 3

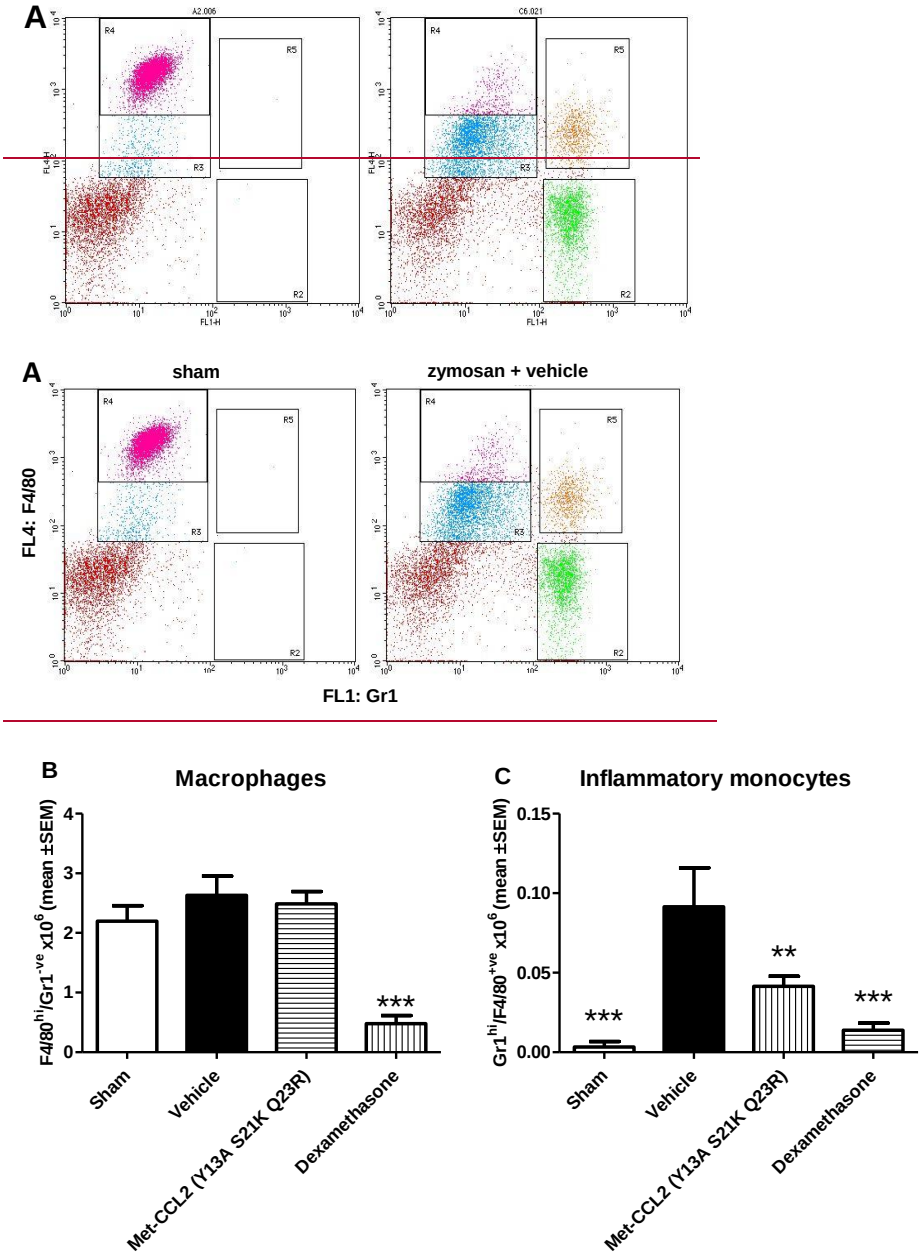
A
A2.006
C6.021
R4
R5
R3
R2
FL4-H
FL1-H
A
sham
zymosan + vehicle
FL4: F4/80
FL1: Gr1
B
Macrophages
F4/80hi/Gr1-ve x10^6 (mean ±SEM)
***
Sham
Vehicle
Met-CCL2 (Y13A S21K Q23R)
Dexamethasone
C
Inflammatory monocytes
Gr1hi/F4/80+ve x10^6 (mean ±SEM)
***
**
***

Figure 4

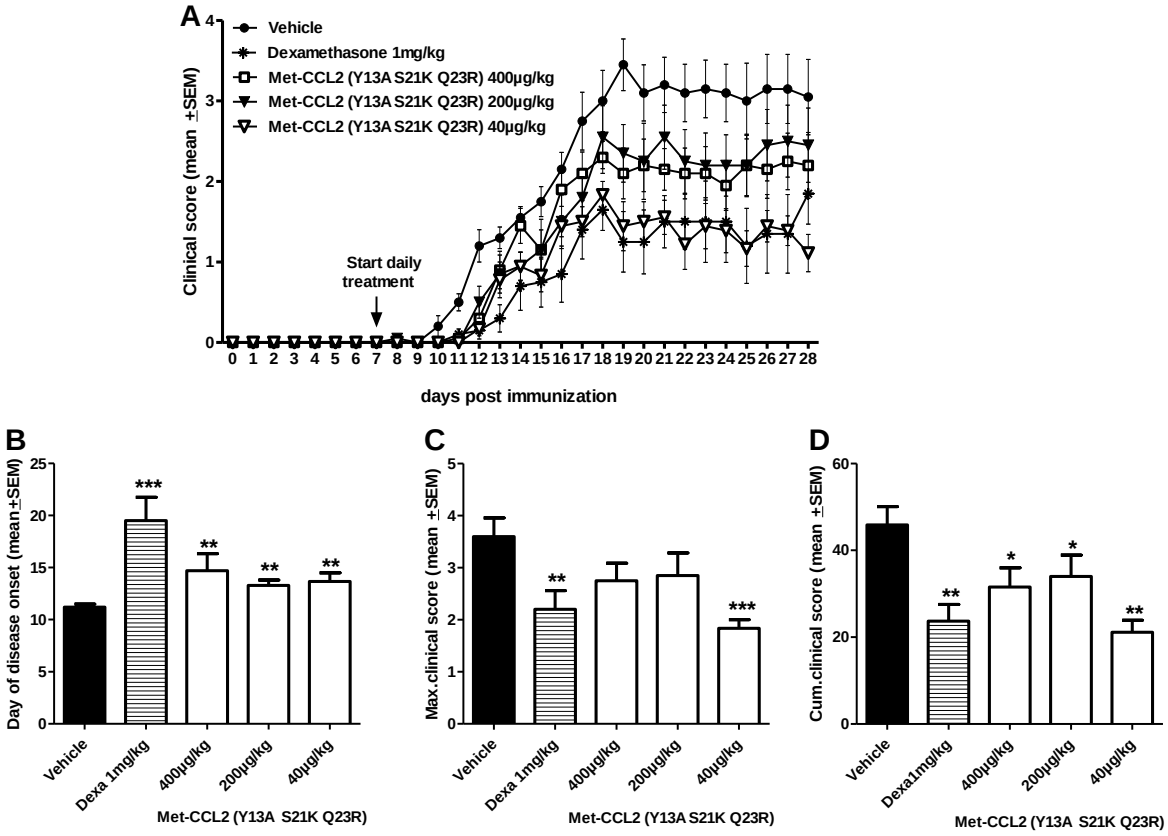
A
Vehicle
Dexamethasone 1mg/kg
Met-CCL2 (Y13A S21K Q23R) 400µg/kg
Met-CCL2 (Y13A S21K Q23R) 200µg/kg
Met-CCL2 (Y13A S21K Q23R) 40µg/kg
Clinical score (mean ±SEM)
Start daily treatment
days post immunization
B
Day of disease onset (mean±SEM)
Vehicle
Dexa 1mg/kg
400µg/kg
200µg/kg
40µg/kg
Met-CCL2 (Y13A S21K Q23R)
C
Max.clinical score (mean ±SEM)
Vehicle
Dexa 1mg/kg
400µg/kg
200µg/kg
40µg/kg
Met-CCL2 (Y13A S21K Q23R)
D
Cum.clinical score (mean ±SEM)
Vehicle
Dexa1mg/kg
400µg/kg
200µg/kg
40µg/kg
Met-CCL2 (Y13A S21K Q23R)

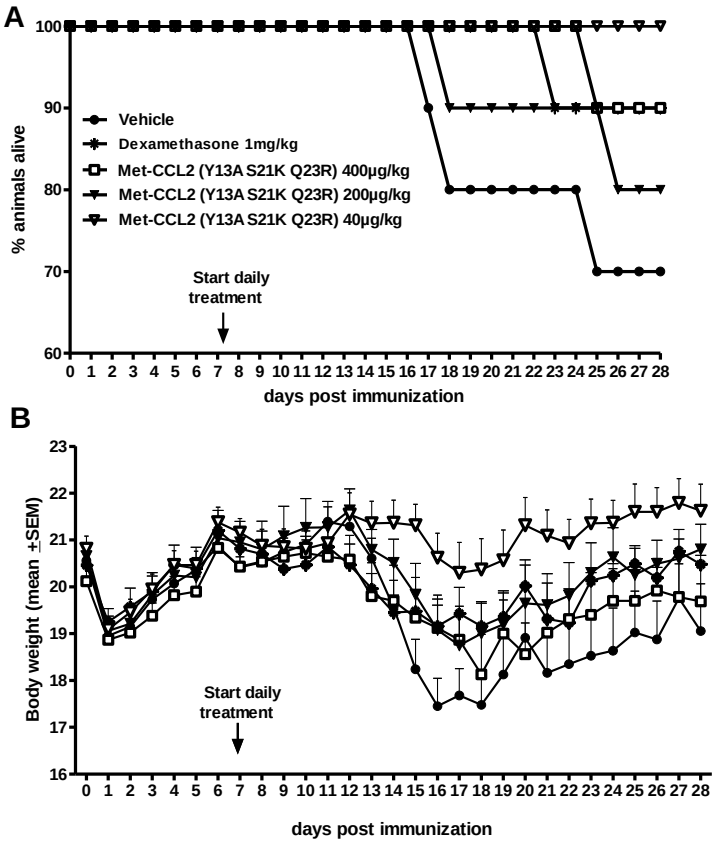
A
% animals alive
Vehicle
Dexamethasone 1mg/kg
Met-CCL2 (Y13A S21K Q23R) 400µg/kg
Met-CCL2 (Y13A S21K Q23R) 200µg/kg
Met-CCL2 (Y13A S21K Q23R) 40µg/kg
Start daily treatment
days post immunization
B
Body weight (mean ±SEM)
Start daily treatment
days post immunization

Figure 5

Figure 6

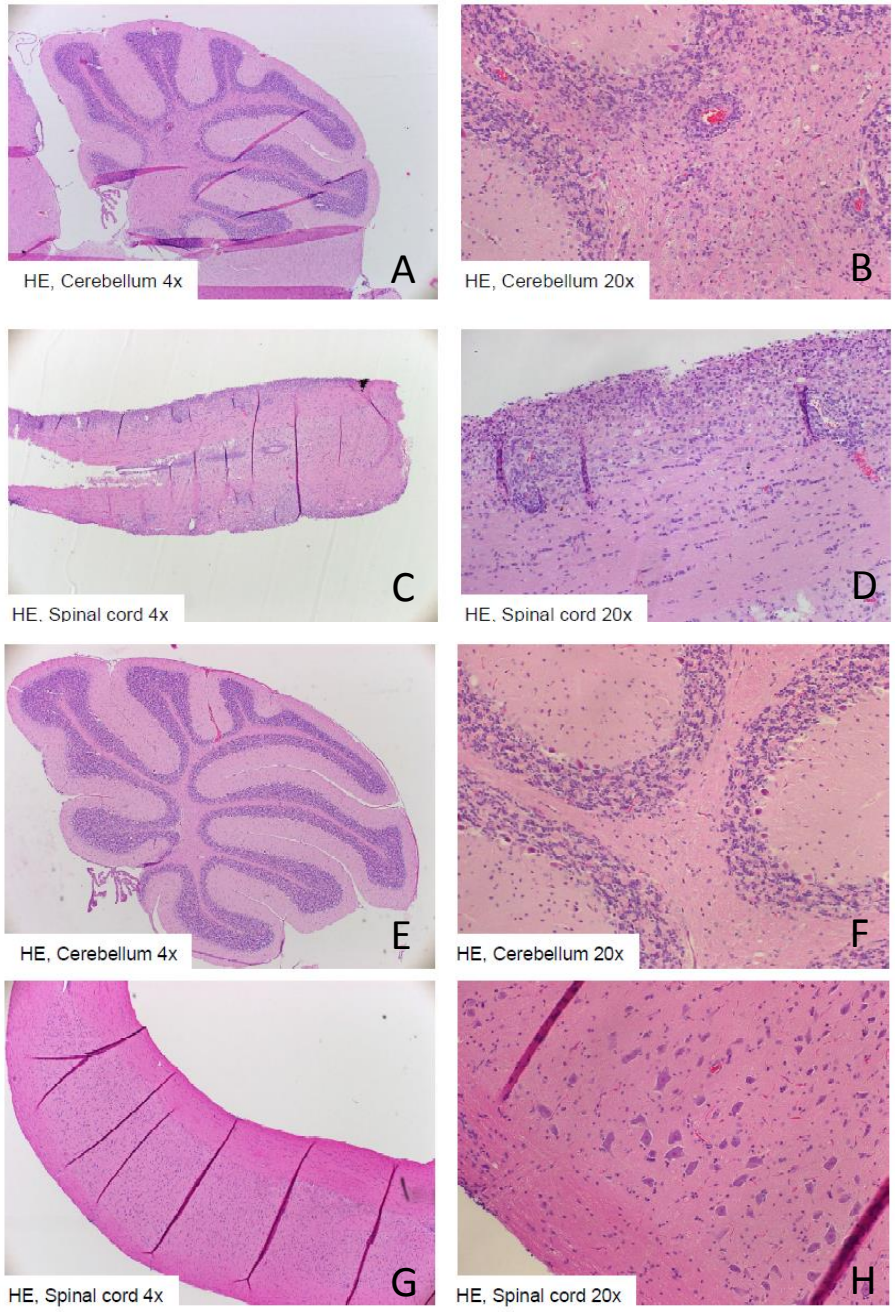
HE, Cerebellum 4x
A
HE, Cerebellum 20x
B
HE, Spinal cord 4x
C
HE, Spinal cord 20x
D
HE, Cerebellum 4x
E
HE, Cerebellum 20x
F
HE, Spinal cord 4x
G
HE, Spinal cord 20x
H

Figure 6

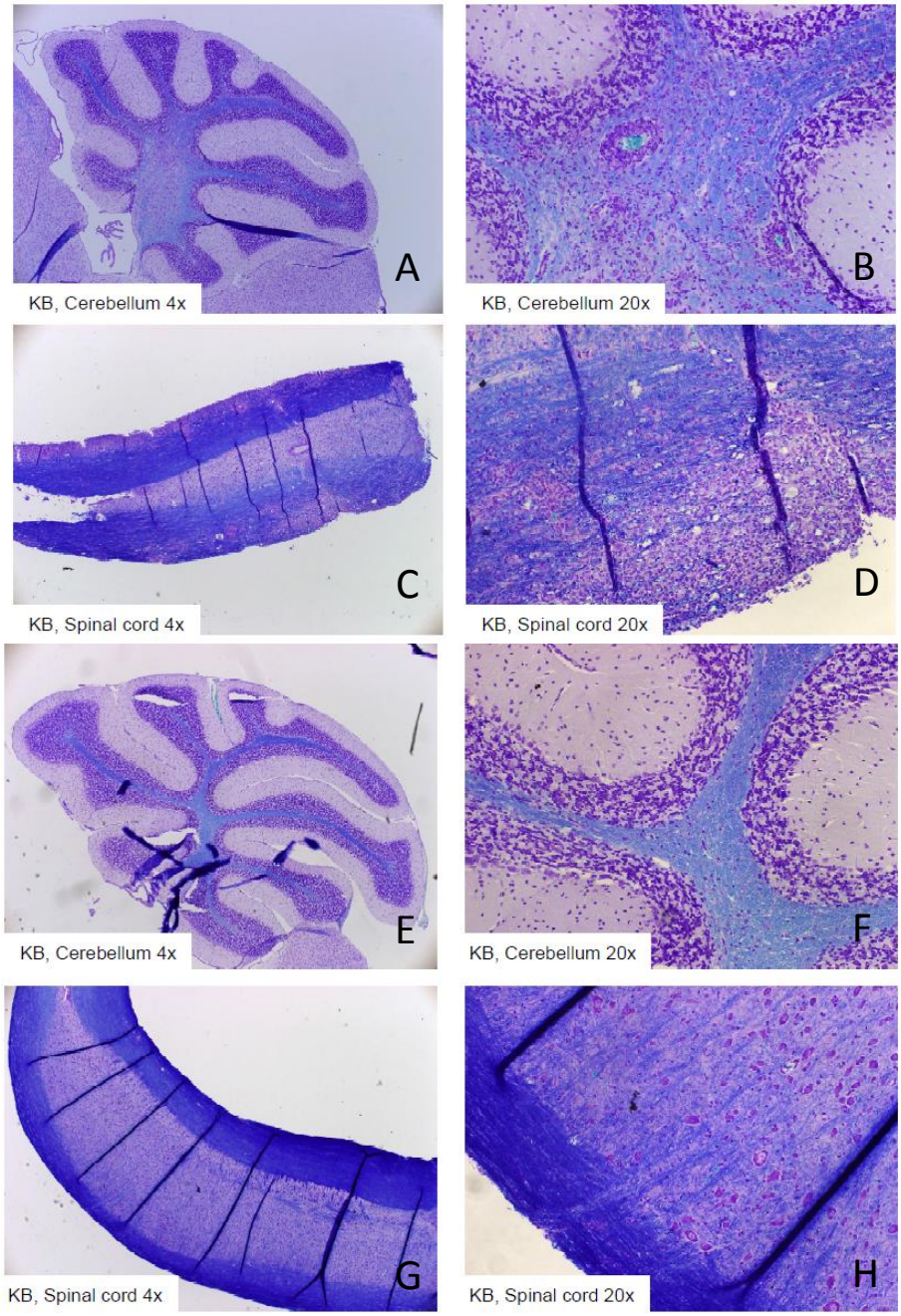
A
KB, Cerebellum 4x
B
KB, Cerebellum 20x
C
KB, Spinal cord 4x
D
KB, Spinal cord 20x
E
KB, Cerebellum 4x
F
KB, Cerebellum 20x
G
KB, Spinal cord 4x
H
KB, Spinal cord 20x